Study of Casson Blood Flow in Stenosed Artery with Magnetic Field and Thermal Diffusion Effects

Nilesh Patel 1, Harshad Patel 2*

1 Research Scholar, Gujarat Technological University, Ahmedabad 382424, Gujarat, India
2* U.V.P.C.E., Ganpat University, Kherva, Gujarat – 384012, India

Corresponding Author: Harshad Patel [2*]

Abstract

In this research paper, unsteady free convective MHD Casson blood flow are studied with stenosis artery. Thermo-diffusion, chemical reaction and heat source/absorption effects are considered. The mathematical modelling of said problems is remodeled into the system of PDE's in cylindrical form with different physical boundary situations. For more impact of physical point of view, the Caputo-Fabrizio fractional ordered derivative is applied on governing momentum, energy, and concentration equations. The Laplace and Finite Hankel transformation is used to finding the analytical expression. From graphical results, it is seen that the thickness of blood is raised with increasing the values of magnetic fields. It is seen that, the Casson fluid parameter tends to improve both blood and magnetic particle velocity. It is also deduced that the heat source tends to raise the heat transfer process whereas thermo-diffusion tends to reduce the mass transfer process.

Keywords: Stenosed artery; Magnetic field; Thermal diffusion; Casson fluid; Magnetic Particles; fractional derivative.

Nomenclature:

Symbol	Physical variables
A_0	Pressure gradient (Systolic)
A_1	Pressure gradient (Diastolic)
$\vec{B}$	Magnetic Field
γ	Casson fluid parameter
ω	Pulsatile frequency
$R=\frac{KN\lambda}{\rho}$	Non – dimensional particle concentration parameter
H_a	Non – dimensional Hartman number
$\emptyset$	Phase angle
F	Inclination angle parameter
D	Differential operator
λ	Relaxation time
R_0	Regular artery radius
L_0	Stenosis Length
$\bar{d}$	Stenosis Location
P	Oscillating pressure gradient

$R_e = \frac{{R_z}^2}{\lambda v}$	Reynolds number
$F = \frac{R_0}{\lambda u_0 g}$	Inclination angle parameter
P_e	Peclet Number
Q_m	Metabolic Heat Source
θ_m	Metabolic Heat absorption
G	Particle mass parameter
ρ	Fluid density
r	Radial coordinator
S	Laplace transform parameter
α	Fractional parameter
σ	Electrical conductivity
$u(r,t)$	velocity of blood
$v(r,t)$	Velocity of the magnetic Particle
N	Magnetic particles number
m	The average mass of magnetic particles
K	Stokes constant
υ	Kinematic viscosity
$\beta = \frac{\mu_{B\sqrt{2\pi_c}}\mu}{\tau_r}$	Casson fluid's material parameter
μ_B	Plastic dynamic viscosity
τ_r	Yield stress
$2\pi_c$	A critical value of this model
$\frac{KN}{\rho}(v-u)$	Force of relative motion between magnetic particles and blood.
S_c	Schmidt number
S_r	Soret parameter
K_c	Chemical reaction parameter
D_m	Mass diffusivity (blood)
K_T	Ratio of thermal diffusion ratio
K_2	Coefficient of Chemical reaction parameter

1. Introduction

Blood flow via arteries is a significant physiological issue that biomedical researchers, physiologists, and therapists are all very interested in Controlling the flow of biological fluids for several surgical procedures. The human circulatory system may be impacted by electromagnetic fields present during such operations. Kollin [1] introduced the concept of electromagnetic fields in the context of medical study, while Korchevskii and Marochnik [2] investigated the external magnet to blood which is travels in human body. ECG patterns collected in a magnetic particle which can deliver the information on blood flow and a non-offensive way for measuring heart performance. Vardanyan [3] looked at the feasibility of using MHD concepts to the reduction and logical treatment of arterial hypertension. BFD problems in stenosis artery has been discussed by many researchers [4-5] Numerous potential applications in hemodynamic have been found thanks to these investigations. Ali et al. [6] discussed the magnetic fields effects on blood flow problems. The purpose of this research is to examine how a magnetic field impacts two-phase blood flow. Pennes [7] published a fundamental study in the late 1940s that established the groundwork for mathematical modelling of heat transfer in biofluid engineering, providing the way for further research into heat transfer in tissues. Furthermore, convection fluxes in hemodynamic and radiative heat transfer in thermal radiation therapy biotechnologies have been studied. Barnothy [8] considered heat transfer effects on blood flow. It is also examining the above research papers; the external magnetic fields tend reduce the heat transfer process. Recently, many researchers find the numerical solutions of magnetic field effects on fluid flow problems with heat transfer and mass transfer in different physical parameter [9-10]. The blood in porous medium is very important phenomena which is applied in many engineering and medical branches. Ganesan and Palani [11] discussed free convective flow of viscous fluid whereas, Takhar et al. [12] considered stagnation area in rotating and translating spherical with Lorentz force.

The two-phase flow model was studied by Abbas et al. [13] with imposing both temperature and velocity slips on the system. The researchers found that when the thermal slip parameter values increased, so did the blood flow temperature profile. They found that thermal slip enhances blood flow heat flux. Khaled and Vafai [14] discussed porous media's importance in flow and heat transport investigations in biological tissues. There is rare research on the topics of blood flow in stenosis artery where fractional-order derivatives are examined. Fractional Calculus more impactful research topic which is used in science and engineering domain. In mathematics, Studying the differentiation and integration with non-integer order mechanisms is expanding fields of fractional calculus. Recently, mathematicians and engineers found a fractional calculus is important concepts in various disciplines, such as electrochemistry, rheology, diffusion etc. The fractional type of derivative has been many effectively applied in many fields like fluid mechanics, biology, medical, etc. The Caputo fractional derivatives are considered in fluid flow problems where Laplace transforms is used to finding the solution of governing equations [15]. The thermos-diffusion effects have been used for isotope separation and in mixture light and medium molecular weight. Mondal et al. [16] and Biswas et al. [17] find the numerical solution of hydrodynamic flow. Recently, Kataria and Patel [18] considered soret effects on MHD flow in porous medium. Maiti et al. [19] examined blood flow using fractional types of derivative with thermal radiation.

2. Novelty of the Research work

In this paper, the fractional time derivative model of Casson blood fluid flow in a stenosed artery is considered. The governing system of equations can be expressed in the fractional time derivative form and derived exact expression of blood velocity, magnetic field velocity, and temperature fields. The exact solutions were computed using LT and HT. Based on these solutions, we were able to calculate numerical results for the axial blood flow velocity, magnetic particle velocity and temperature profiles and presented through graphs. Mathematical Analysis of Bio magnetic fluid flow and Heat Transfer in Stenosed arteries is useful for improving human health. Magnetic field is used to reduce the blood viscosity which can be helpful for controlling the rate of blood flow. Due to this concept, we improve the health condition of patient which is suffer with cardiovascular disease. It is important to blood flow through stenosed artery for understanding of circulatory disorders and hoping that this study is also useful for development and treatment of blood circulation disorders in humans. Hence, the proposed research works is applicable for solving many cardiovascular diseases which is disturb the regular rate of blood flow circulations.

3. Mathematical Formulation & Solution

The focus of the current research is on unsteady fluid flow in an angled stenosed artery, which is outlined in Figure 1 and $z-$axis is axial direction, while $r-$axis indicates radial direction. The model was developed using the incompressible Casson blood fluid that is accelerated through fluctuating pressure.

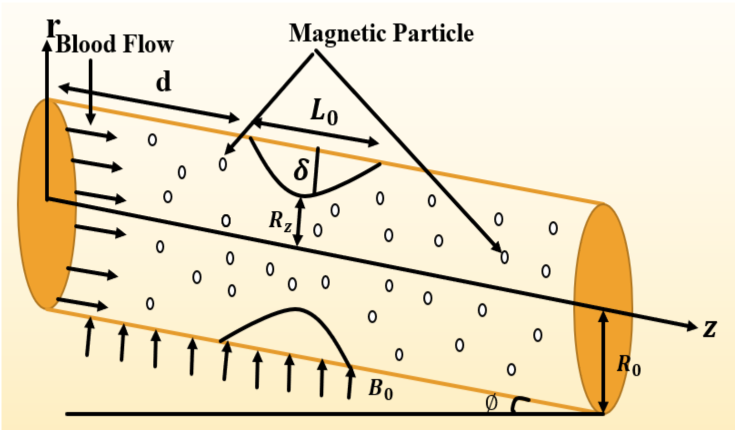

Fig. 1: Physical Sketch of the inclined stenosed artery

Fig. 1 displays a graphic of the magnetic field B_0 that is delivered to the body to increase blood flow, with the generated magnetic field considered to be minimal. At time zero, both the blood and the magnetic particles were at rest. Blood flow and heat transfer are modelled using the Navier-Stokes and energy equations, while the magnetic field is described by Maxwell's relations and particle motion is governed by Newton's second law.

Unsteady motion in a cylinder with axis symmetry and radius R_0, due to a pressure gradient

$$-\frac{\partial P}{\partial z} = A_0 + A_1 \mathrm{Cos}\,(\omega t), A_0 > 0 \tag{1}$$

Geometrically, the stenosis is symmetric but non-symmetric in the radial direction, can be described as

$$R_z = \begin{cases} \{R_0 - R_0\xi\{L_0^{q-1}(\bar{z}-\bar{d}) - (\bar{z}-\bar{d})^q\}\}, & \bar{d} < \bar{z} < \bar{d} + L_0 \\ R_0 & \text{otherwise} \end{cases} \tag{2}$$

Were, $\xi = \frac{\delta q^{q-1}}{R_0 L_0^q (q-1)}$, $\frac{\delta}{R_0} < 1$ and $\bar{z} = \frac{d+L_0}{\frac{1}{q^{q-1}}}$,

R_z and R_0 represent the stenosed and un-stenosed radius of the artery, L_0 represents the stenosis's length, and $\bar{d}$ represents its position. $q \geq 2$ indicate the shape of stenosis.

The governing equations in cylindrical form are as

$$\frac{\partial u}{\partial t} = -\frac{1}{\rho}\frac{\partial p}{\partial z} + v\left(1+\frac{1}{\beta}\right)\left(\frac{\partial^2 u}{\partial r^2} + \frac{1}{r}\frac{\partial u}{\partial r}\right) - \frac{KN}{\rho}(v-u) - \frac{\sigma\beta_0^2 \sin\theta}{\rho}u + \frac{g\beta}{\rho}(T-T_\infty) + + \frac{g\beta}{\rho}(C-C_\infty) \tag{3}$$

The magnetic particles are governed by Newton's second law which can be written as,

$$m\frac{\partial v}{\partial t} = K(u-v) \tag{4}$$

The energy equation in the cylindrical coordinate can be written as

$$\frac{\partial T}{\partial t} = \frac{K_1}{\rho C_p}\left(\frac{\partial^2 T}{\partial r^2} + \frac{1}{r}\frac{\partial T}{\partial r}\right) + \frac{Q_m + \theta_m}{\rho C_p} \tag{5}$$

Concentration equation can be written as

$$\frac{\partial C}{\partial t} = D_m\left(\frac{\partial^2 C}{\partial r^2} + \frac{1}{r}\frac{\partial C}{\partial r}\right) + \frac{D_m K_T}{T_\infty}\left(\frac{\partial^2 T}{\partial r^2} + \frac{1}{r}\frac{\partial T}{\partial r}\right) - K_2(C - C_\infty) \tag{6}$$

The time-fractional model, equation (3) to equation (6) will be multiplied by $\lambda = \sqrt{\frac{R_0\rho}{A_0}}$.

$$\lambda^{\alpha}D_t^{\alpha}u = -\frac{\lambda}{\rho}\left(A_0 + A_1\cos(\omega t)\right) + \lambda v\left(1+\frac{1}{\beta}\right)\left(\frac{\partial^2 u}{\partial r^2} + \frac{1}{r}\frac{\partial u}{\partial r}\right) + \frac{KN\lambda}{\rho}(v-u) - \frac{\sigma\beta_0^2\sin\theta\lambda}{\rho}u + g\lambda\sin\phi + \lambda g\beta_T(T-T_\infty) + \lambda g\beta_C(C-C_\infty) \quad (7)$$

$$\lambda^{\alpha}D_t^{\alpha}v = \frac{K\lambda}{m}(u-v) \quad (8)$$

$$\lambda^{\alpha}D_t^{\alpha}T = \frac{K\lambda}{\rho C_p}\left(\frac{\partial^2 T}{\partial r^2} + \frac{1}{r}\frac{\partial T}{\partial r}\right) + \frac{Q_m+\theta_m}{\rho C_p} \quad (9)$$

$$\lambda^{\alpha}D_t^{\alpha}C = D_m\lambda\left(\frac{\partial^2 C}{\partial r^2} + \frac{1}{r}\frac{\partial C}{\partial r}\right) + \frac{\lambda D_m K_T}{T_\infty}\left(\frac{\partial^2 T}{\partial r^2} + \frac{1}{r}\frac{\partial T}{\partial r}\right) - K_2(C-C_\infty) \quad - \quad (10)$$

Where, Caputo-Fabrizio operator is

$$^{CF}D_t^{\alpha}u(r,t) = \frac{1}{1-\alpha}\int_0^t \exp\left(-\frac{\alpha(t-\tau)}{1-\alpha}\right)\frac{\partial u(r,\tau)}{\partial \tau}\,d\tau \quad (11)$$

The LT of Caputo-Fabrizio time fractional can be express as

$$L\left\{^{CF}D_t^{\alpha}u(r,t)\right\} = \frac{sL\{u(r,t)-u(r,0)\}}{(1-\alpha)\,s+\alpha} \quad (12)$$

With α $(0 < \alpha < 1)$.

The initial and boundary condition of the blood and magnetic particle, the stenosed artery of Radius R_z are

$$u(r,0) = 0,\ v(r,0) = 0,\ C(r,0) = 0\ \&\ T(r,0) = 0 \text{ at } r \in [0, R_z]$$

$$u(r,t) = 0,\ v(r,t) = 0,\ C(r,t) = 0\ \&\ T(r,t) = 0 \text{ at } r = R_z \quad (13)$$

The following dimensionless parameters can be introduced,

$$r^* = \frac{r}{R_0},\ t^* = \frac{t}{\lambda},\ u^* = \frac{u}{u_0},\ A_0{}^* = \frac{\lambda A_0}{\rho u_0},\ A_1{}^* = \frac{\lambda A_1}{\rho u_0},\ g^* = \frac{g}{\frac{u_0^2}{R_0}}$$

$$\theta = \frac{T-T_\omega}{T_\omega - T_\infty},\ P_r = \frac{\mu C_p}{k},\ R_e = \frac{R_0 u_0}{v},\ P_e = R_e.P_r,\ B_0{}^* = \frac{\lambda B_0}{\rho u_0}$$

$$S_c = \frac{v}{D_m},\ S_r = \frac{D_m K_T(T_\omega - T_\infty)}{v T_\infty (C_\omega - C_\infty)},\ C = \frac{C - C_\omega}{C_\omega - C_\infty},\ Q_m = \frac{R_0\overline{Q_m}}{u_0\rho c_p(T_\omega - T_\infty)},\ \theta_m = \frac{R_0\overline{\theta_m}}{u_0\rho c_p(T_\omega - T_\infty)} \quad (14)$$

Introducing the dimensionless parameter, the equations (7) to (10) and (13) can be written as,

$$D_t^{\alpha}u = A_0 + A_1\cos(\omega t) + \beta_1\left[\frac{\partial^2 u}{\partial r^2} + \frac{1}{r}\frac{\partial u}{\partial r}\right] + R(v-u) - M^2u + Gr\theta + Gm\,C + \frac{\sin\phi}{F} \quad (15)$$

$$GD_t^{\alpha}v = u - v \quad (16)$$

$$P_eD_t^{\alpha}\theta = \left(\frac{\partial^2 \theta}{\partial r^2} + \frac{1}{r}\frac{\partial \theta}{\partial r}\right) + P_e(Q_m + \theta_m) \quad (17)$$

$$R_eS_c\,C = \left(\frac{\partial^2 C}{\partial r^2} + \frac{1}{r}\frac{\partial C}{\partial r}\right) + S_r\,S_c\left(\frac{\partial^2 \theta}{\partial r^2} + \frac{1}{r}\frac{\partial \theta}{\partial r}\right) - S_c\,K_c\,R_e^2C \quad (18)$$

With,

$$u\left(\frac{r}{R_z},0\right)=0\,,v\left(\frac{r}{R_z},0\right)=0\,,\theta\left(\frac{r}{R_z},0\right)=0\ \&\ C\left(\frac{r}{R_z},0\right)=0\ \text{ at } \frac{r}{R_z}\in[\,0\,,1]$$

$$u\left(\frac{r}{R_z},t\right)=0\,,v\left(\frac{r}{R_z},t\right)=0\,,\theta\left(\frac{r}{R_z},t\right)=0\ \&\ C\left(\frac{r}{R_z},t\right)\ \text{ at } \frac{r}{R_z}\ =\ 1 \tag{19}$$

3.1 Solution of the Problem

Now, the LT is a well-suited technique. After the transformation process, we obtain the equations (17) can be written as,

$$P_e\frac{S\,\bar{\theta}(r,s)}{S+\alpha(1-s)}=\left[\frac{\partial^2\bar{\theta}(r,s)}{\partial r^2}+\frac{1}{r}\frac{\partial\bar{\theta}(r,s)}{\partial r}\right]+P_e\frac{Q_m+\theta_m}{S} \tag{20}$$

With boundary condition $\bar{\theta}(1,s)=0$

Applying Finite Hankel transformation of order zero in equations (20) with boundary condition (19), the following equation can be obtained.

$$P_e\frac{S\,\overline{\theta_H}(r_n,s)}{S+\alpha(1-s)}=-r_n\overline{\theta_H}(r_n,s)+P_e\frac{Q_m+\theta_m}{S}.\frac{J_1(r_n)}{r_n} \tag{21}$$

$$\overline{\theta_H}(r_n,s)=\frac{P_e\,(Q_m+\theta_m)}{S\left[r_n+P_e\frac{S}{S+\alpha(1-s)}\right]}.\frac{J_1(r_n)}{r_n} \tag{22}$$

Now, rearrange the equation (22)

$$\overline{\theta_H}(r_n,s)=\left[\frac{1}{S+B_{15}}B_{13}+\frac{1}{S-B_{15}}B_{14}\right]\frac{J_1(r_n)}{r_n} \tag{23}$$

Similarly, we process for Concentration equation (18), we get

$$R_eS_c\frac{S\,\bar{C}(r,s)}{S+\alpha(1-s)}=\left(\frac{\partial^2\bar{C}(r,s)}{\partial r^2}+\frac{1}{r}\frac{\partial\bar{C}(r,s)}{\partial r}\right)+S_r\,S_c\left(\frac{\partial^2\bar{\theta}(r,s)}{\partial r^2}+\frac{1}{r}\frac{\partial\bar{\theta}(r,s)}{\partial r}\right)-S_c\,K_c\,R_e^2\,\bar{C}(r,s) \tag{24}$$

With boundary condition $\bar{C}(1,s)=0$.

Applying Finite Hankel transformation of order zero in equations (24) with boundary condition (19), the following equation can be obtained.

$$R_eS_c\frac{S\,\overline{C_H}(r,s)}{S+\alpha(1-s)}=-r_n\overline{C_H}(r_n,s)+S_r\,S_c\,(-r_n)\overline{\theta_H}(r_n,s)-S_c\,K_c\,R_e^2\,\overline{C_H}(r_n,s) \tag{25}$$

$$R_eS_c\frac{S\,\overline{C_H}(r,s)}{S+\alpha(1-s)}=-r_n\overline{C_H}(r_n,s)+S_r\,S_c\,(-r_n)\frac{P_e\,(Q_m+\theta_m)}{S\left[r_n+P_e\frac{S}{S+\alpha(1-s)}\right]}.\frac{J_1(r_n)}{r_n}-S_c\,K_c\,R_e^2\,\overline{C_H}(r_n,s) \tag{26}$$

$$\left[\frac{R_eS_c.S}{S+\alpha(1-s)}+r_n+S_c\,K_c\,R_e^2\right]\overline{C_H}(r,s)=-r_nS_r\,S_c\left[\frac{P_e\,(Q_m+\theta_m)}{S\left[r_n+P_e\frac{S}{S+\alpha(1-s)}\right]}\right].\frac{J_1(r_n)}{r_n} \tag{27}$$

$$\overline{C_H}(r,s)=-\frac{S_r\,S_c\,r_nP_e\,(Q_m+\theta_m)}{\left(S\left[r_n+P_e\frac{S}{S+\alpha(1-s)}\right]\right)\left[\frac{R_eS_c.S}{S+\alpha(1-s)}+r_n+S_c\,K_c\,R_e^2\right]}.\frac{J_1(r_n)}{r_n} \tag{28}$$

Now, rearrange the equation (28)

$$\overline{C_H}(r,s) = \frac{B_{16}}{\left(S\left[B_{17}+P_e\frac{S}{S+\alpha(1-s)}\right]\right)\left[\frac{B_{19}.S}{S+\alpha(1-s)}+r_n+B_{18}\right]}.\frac{J_1(r_n)}{r_n} \tag{29}$$

$$\overline{C_H}(r,s) = \frac{B_{16}\,(S+\alpha(1-S))^2}{S\,(B_{17}S+B_{17}\alpha-B_{17}\alpha S+P_eS)(B_{19}S+B_{18}\alpha+B_{18}S-B_{18}\alpha S)}.\frac{J_1(r_n)}{r_n} \tag{30}$$

$$\overline{C_H}(r,s) = \frac{B_{16}\,(S+\alpha(1-S))^2}{S\,((B_{17}-B_{17}\alpha+P_e)S+B_{17}\alpha)((B_{19}+B_{18}-B_{18}\alpha)S+B_{18}\alpha)}.\frac{J_1(r_n)}{r_n} \tag{31}$$

$$\overline{C_H}(r,s) = \frac{B_{16}\,(S+\alpha(1-S))^2}{S\,(B_{20}S+B_{22})(B_{21}S+B_{23})}.\frac{J_1(r_n)}{r_n} \tag{32}$$

$$\overline{C_H}(r,s) = \frac{B_{16}}{B_{20}.B_{21}}\frac{(\alpha^2+2\alpha(1-\alpha)S+(1-\alpha)^2S^2)}{S\left(S+\frac{B_{22}}{B_{20}}\right)\left(S+\frac{B_{23}}{B_{21}}\right)}.\frac{J_1(r_n)}{r_n} \tag{33}$$

$$\overline{C_H}(r,s) = \frac{B_{16}}{B_{20}.B_{21}}\frac{(\alpha^2+2\alpha(1-\alpha)S+(1-\alpha)^2S^2)}{S\left(S+\frac{B_{22}}{B_{20}}\right)\left(S+\frac{B_{23}}{B_{21}}\right)}.\frac{J_1(r_n)}{r_n} \tag{34}$$

$$\overline{C_H}(r,s) = \frac{B_{24}\,(\alpha^2+B_{25}S+B_{26}S^2)}{S\,(S+B_{27})\,(S+B_{28})}.\frac{J_1(r_n)}{r_n} \tag{35}$$

$$\overline{C_H}(r,s) = \left(\frac{B_{29}}{S}+\frac{B_{30}}{S+B_{27}}+\frac{B_{29}}{S+B_{28}}\right).\frac{J_1(r_n)}{r_n} \tag{36}$$

Now applying the Laplace transform of equations (15) and (16) can be express as,

$$\frac{S\,\bar{u}(r,s)}{S+\alpha(1-s)} = \frac{A_0}{S}+\frac{A_1S}{s^2+\omega^2}+\beta_1\left(\frac{\partial^2\bar{u}(r,s)}{\partial r^2}+\frac{1}{r}\frac{\partial\bar{u}(r,s)}{\partial r}\right)+R\bar{v}-(R+Ha^2)\bar{u}(r,s)+Gr\bar{\theta}+Gm\,\bar{C}+\frac{\sin\emptyset}{SF} \tag{37}$$

$$G\,\frac{S\,\bar{v}(r,s)}{S+\alpha(1-s)} = \bar{u}(r,s)-\bar{v}(r,s) \tag{38}$$

$$\bar{v}(r,s) = \frac{S+\alpha(1-\alpha)}{GS+S+\alpha(1-s)}\,\bar{u}(r,s) \tag{39}$$

With boundary condition $\bar{u}(1,s)=0,\ \bar{v}(1,s)=0$.

Input the equation (23), (36) and (39) in (37), the following equation can be obtained,

$$\left[\frac{s}{S+\alpha(1-S)}-R\left(\frac{S+\alpha(1-\alpha)}{GS+S+\alpha(1-s)}\right)+R+Ha^2\right]\bar{u}(r,s) = \frac{A_0}{S}+\frac{A_1S}{s^2+\omega^2}+\beta_1\left(\frac{\partial^2\bar{u}}{\partial r^2}+\frac{1}{r}\frac{\partial\bar{u}}{\partial r}\right)+Gr\bar{\theta}+Gm\,\bar{C}+\frac{\sin\phi}{SF} \tag{40}$$

Applying Finite Hankel transformation of order zero in equations (40) with boundary condition (19), the following equation can be obtained.

$$\left[\frac{s}{S+\alpha(1-S)}-R\left(\frac{S+\alpha(1-\alpha)}{GS+S+\alpha(1-s)}\right)+R+Ha^2\right]\overline{u_H}(r_n,s) = \left[\frac{A_0}{S}+\frac{A_1S}{s^2+\omega^2}+\frac{\sin\phi}{SF}\right]\frac{J_1(r_n)}{r_n}-r_n\beta_1\overline{u_H}(r_n,s)+Gr\left[\frac{1}{S+B_{15}}B_{13}+\frac{1}{S-B_{15}}B_{14}\right]\frac{J_1(r_n)}{r_n}+Gm\left(\frac{B_{29}}{S}+\frac{B_{30}}{S+B_{27}}+\frac{B_{29}}{S+B_{28}}\right).\frac{J_1(r_n)}{r_n} \tag{41}$$

$$\overline{u_H}(r_n,s) = \frac{S^2B_5+SB_6+\alpha^2}{S^2B_2+SB_3+B_4}\left[\frac{1}{S}\left(A_0+\frac{\sin\phi}{F}+\frac{A_1S}{s^2+\omega^2}\right)\right]\frac{J_1(r_n)}{r_n}+Gr\left[\frac{1}{S+B_{15}}B_{13}+\frac{1}{S-B_{15}}B_{14}\right]\frac{J_1(r_n)}{r_n}+Gm\left(\frac{B_{29}}{S}+\frac{B_{30}}{S+B_{27}}+\frac{B_{29}}{S+B_{28}}\right).\frac{J_1(r_n)}{r_n} \tag{42}$$

$$\therefore \overline{u_H}(r_n,s) = \left[\frac{B_9}{S-B_7}+\frac{B_{10}}{S-B_8}\right]\left[\frac{1}{S}\left(A_0+\frac{\sin\phi}{F}+\frac{A_1 S}{s^2+\omega^2}\right)\right]\frac{J_1(r_n)}{r_n}+Gr\left[\frac{1}{S+B_{15}}B_{13}+\frac{1}{S-B_{15}}B_{14}\right]\frac{J_1(r_n)}{r_n}+Gm\left(\frac{B_{29}}{S}+\frac{B_{30}}{S+B_{27}}+\frac{B_{29}}{S+B_{28}}\right).\frac{J_1(r_n)}{r_n} \tag{43}$$

$$\therefore \overline{u_H}(r_n,s) = \left(A_0+\frac{\sin\phi}{F}\right)\left[\frac{S^{-1}}{S-B_7}B_9+\frac{S^{-1}}{S-B_8}B_{10}\right]\frac{J_1(r_n)}{r_n}+\frac{A_1 S}{s^2+\omega^2}\left[\frac{1}{S-B_7}B_9+\frac{1}{S-B_8}B_{10}\right]\frac{J_1(r_n)}{r_n}+Gr\left[\frac{1}{S+B_{15}}B_{13}+\frac{1}{S-B_{15}}B_{14}\right]\frac{J_1(r_n)}{r_n}+Gm\left(\frac{B_{29}}{S}+\frac{B_{30}}{S+B_{27}}+\frac{B_{29}}{S+B_{28}}\right).\frac{J_1(r_n)}{r_n} \tag{44}$$

Where, $\overline{u_H}(r_n,s) = \int_0^1 r.\bar{u}(r,s)J_0(r_n,r)\,dr$ represents the finite Hankel transformation of the velocity and temperature function.

$$\bar{u}(r,s) = LT[\bar{u}(r,t)],\ \bar{\theta}(r,s) = LT[\bar{\theta}(r,t)] \text{ and } \bar{C}(r,s) = LT[\bar{C}(r,t)] \tag{45}$$

And $r_n, n = 1,2,3, \ldots..$ are the positive roots of an equation $J_0(x) = 0$.

The inverse Laplace transform of the image function can be written as,

$$LT^{-1}\left[\frac{1}{S^{\omega}+y}\right] = F_{\omega}(-y,t) = \sum_{n=0}^{\infty}\frac{(-y)^n t^{(n+1)w-1}}{\Gamma((n+1)w)}\ ;\ \omega > 0 \tag{46}$$

$$LT^{-1}\left[\frac{S^z}{S^w+y}\right] = R_{w,z}(-y,t) = \sum_{n=0}^{\infty}\frac{(-y)^n t^{(n+1)w-1-z}}{\Gamma((n+1)w-z)}\ ;\ Re(w-z) > 0 \tag{47}$$

Now, Applying the Inverse Laplace transform of equations (23), (36) and (44) are

$$\therefore \overline{\theta_H}(r_n,t) = \frac{J_1(r_n)}{r_n}\left[B_{13}e^{-B_{15}t}+\frac{B_{14}}{B_{15}}(1-e^{-B_{15}t})\right] = \frac{J_1(r_n)}{r_n}[B_{13}F_1(-B_{15},t)+B_{14}R_{i-1}(-B_{15},t)] \tag{48}$$

$$\therefore \overline{C_H}(r_n,t) = \frac{J_1(r_n)}{r_n}[B_{29}+B_{30}e^{-B_{27}t}+B_{31}e^{-B_{31}t}] \tag{49}$$

$$\therefore \overline{u_H}(r_n,t) = \frac{J_1(r_n)}{r_n}\left[(e^{B_7 t}-1)\left(\frac{A_0}{B_7}B_9+\frac{B_9\sin\phi}{B_7 F}\right)+(e^{B_8 t}-1)\left(\frac{A_0}{B_8}B_{10}+\frac{B_{10}\sin\phi}{B_8 F}\right)+A_1B_9e^{B_7 t}*\cos(\omega t)+A_1B_{10}e^{B_8 t}*\cos(\omega t)\right]+Gr\frac{J_1(r_n)}{r_n}[B_{13}F_1(-B_{15},t)+B_{14}R_{i-1}(-B_{15},t)]+Gm\frac{J_1(r_n)}{r_n}[B_{29}+B_{30}e^{-B_{27}t}+B_{31}e^{-B_{31}t}] \tag{50}$$

The exact expression of blood velocity, Temperature and Concentration profiles are obtained by taking the Inverse Hankel transformation of equations (48) - (50), we get

$$\theta(r,t) = 2\sum_{n=1}^{\infty}\frac{J_0\left(\frac{r}{r_z}r_n\right)}{r_nJ_1^2(r_n)}\times\theta_H(r_n,t) \tag{51}$$

$$\theta(r,t) = 2\sum_{n=1}^{\infty}\frac{J_0\left(\frac{r}{r_z}r_n\right)}{r_nJ_1^2(r_n)}\times\left[B_{13}e^{-B_{15}t}+\frac{B_{14}}{B_{15}}(1-e^{-B_{15}t})\right] \tag{52}$$

$$C(r,t) = 2\sum_{n=1}^{\infty}\frac{J_0\left(\frac{r}{r_z}r_n\right)}{r_nJ_1^2(r_n)}\times C_H(r_n,t) \tag{53}$$

$$C(r,t) = 2\sum_{n=1}^{\infty}\frac{J_0\left(\frac{r}{r_z}r_n\right)}{r_nJ_1^2(r_n)}\times[B_{29}+B_{30}e^{-B_{27}t}+B_{31}e^{-B_{31}t}] \tag{54}$$

$$u(r,t) = 2\sum_{n=1}^{\infty}\frac{J_0\left(\frac{r}{r_z}r_n\right)}{r_n J_1^2(r_n)}\times u_H(r_n,t) + Gr\,2\sum_{n=1}^{\infty}\frac{J_0\left(\frac{r}{r_z}r_n\right)}{r_n J_1^2(r_n)}\times \theta_H(r_n,t) + Gm2\sum_{n=1}^{\infty}\frac{J_0\left(\frac{r}{r_z}r_n\right)}{r_n J_1^2(r_n)}\times C_H(r_n,t) \tag{55}$$

$$u(r,t) = 2\sum_{n=1}^{\infty}\frac{J_0\left(\frac{r}{r_z}r_n\right)}{r_n J_1^2(r_n)}\left[(e^{B_7 t}-1)\left(\frac{A_0}{B_7}B_9+\frac{B_9\sin\phi}{B_7F}\right)+(e^{B_8 t}-1)\left(\frac{A_0}{B_8}B_{10}+\frac{B_{10}\sin\phi}{B_8F}\right)+\quad A_1B_9e^{B_7 t}*\cos(\omega t)+ A_1B_{10}e^{B_8 t}*\cos(\omega t)\right]+Gr\,2\sum_{n=1}^{\infty}\frac{J_0\left(\frac{r}{r_z}r_n\right)}{r_n J_1^2(r_n)}\times\left[B_{13}e^{-B_{15}t}+\frac{B_{14}}{B_{15}}(1-e^{-B_{15}t})\right]+Gm2\sum_{n=1}^{\infty}\frac{J_0\left(\frac{r}{r_z}r_n\right)}{r_n J_1^2(r_n)}\times[B_{29}+ B_{30}e^{-B_{27}t}+B_{31}e^{-B_{31}t}] \tag{56}$$

The magnetic particle velocity can be obtained from equation (39)

$$v(r,t) = B_{33}(1-B_{32})[u(r,t)*e^{B_{12}t}],\ 0<\alpha<1 \tag{57}$$

4. Numerical Results and Analysis

By analysing the effects of different parameter on blood and magnetic particle velocities, energy and concentration profiles, the numerical result is obtained and represent through the Fig. 2 to 20. Figure 2 to 3 show the effects of A_0 and A_1 on blood velocity where another parameter is fixed. It is seen that the motion of the blood improves with increasing values of the parameters. Physically, when we increase the pressure gradient, fluid is accelerated due to this reason the velocity of the blood flow is increased. The Casson fluid parameter effects on both velocities which is describe in Fig. 4 to 5. It is seen that both velocities increase with increasing in the parameter. Casson's behaviour is more important in small arteries because of the possibility of red blood cell collection and cell distribution there owing to rotation of the artery's axis.

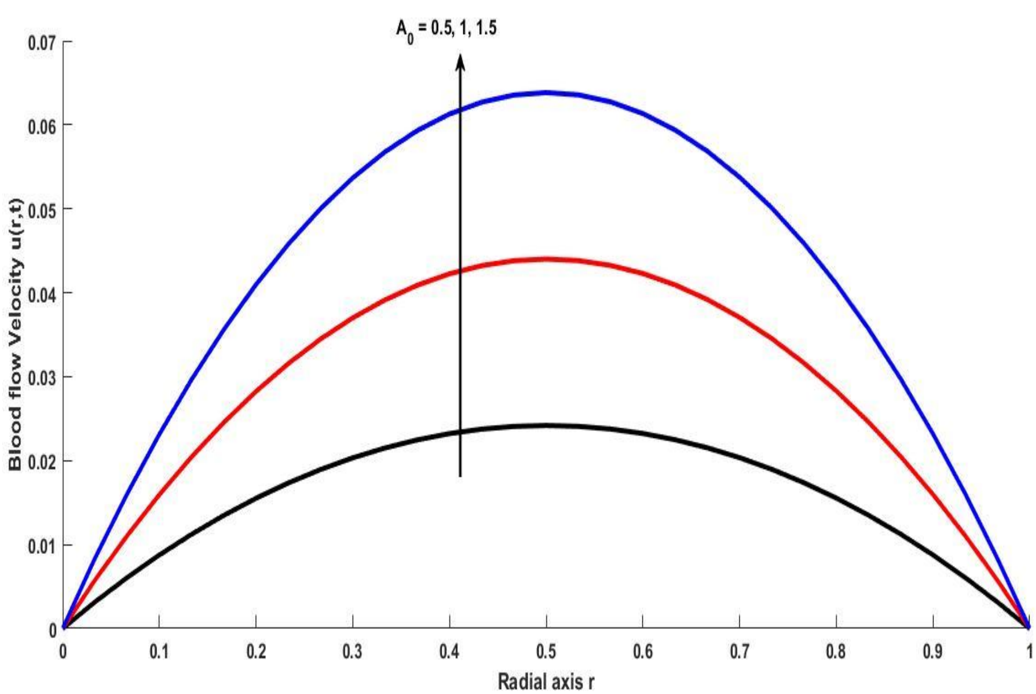

Fig. 2: A_0 on Blood Velocity

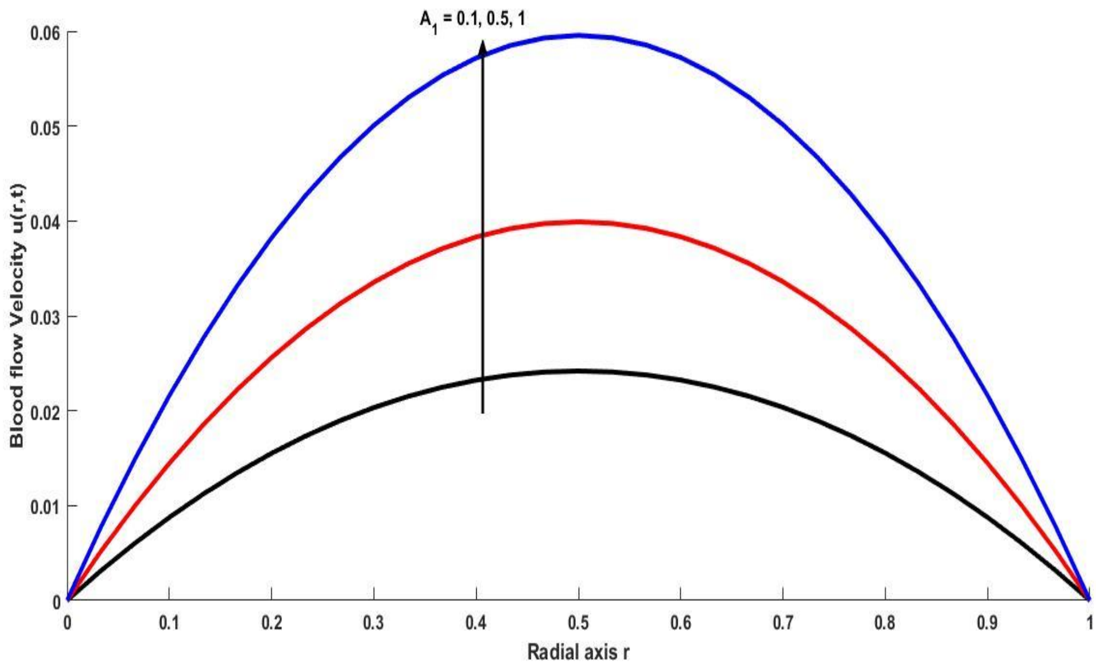

Fig. 3: A_1 on Blood Velocity

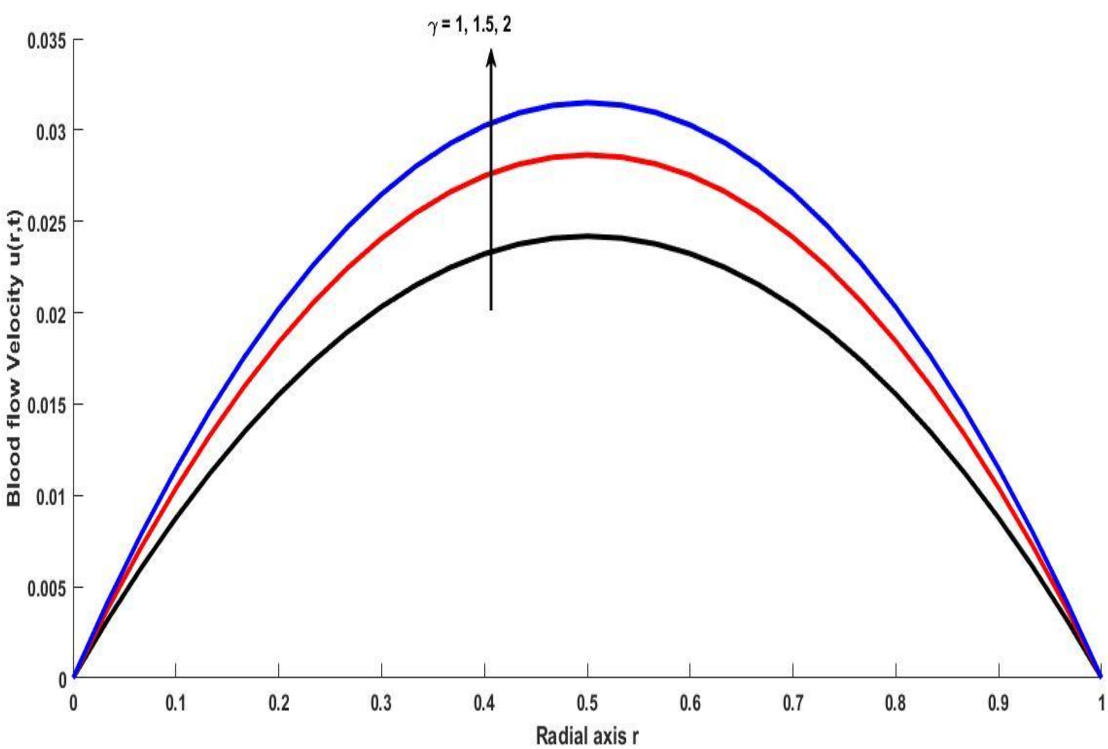

Fig. 4: γ on Blood Velocity

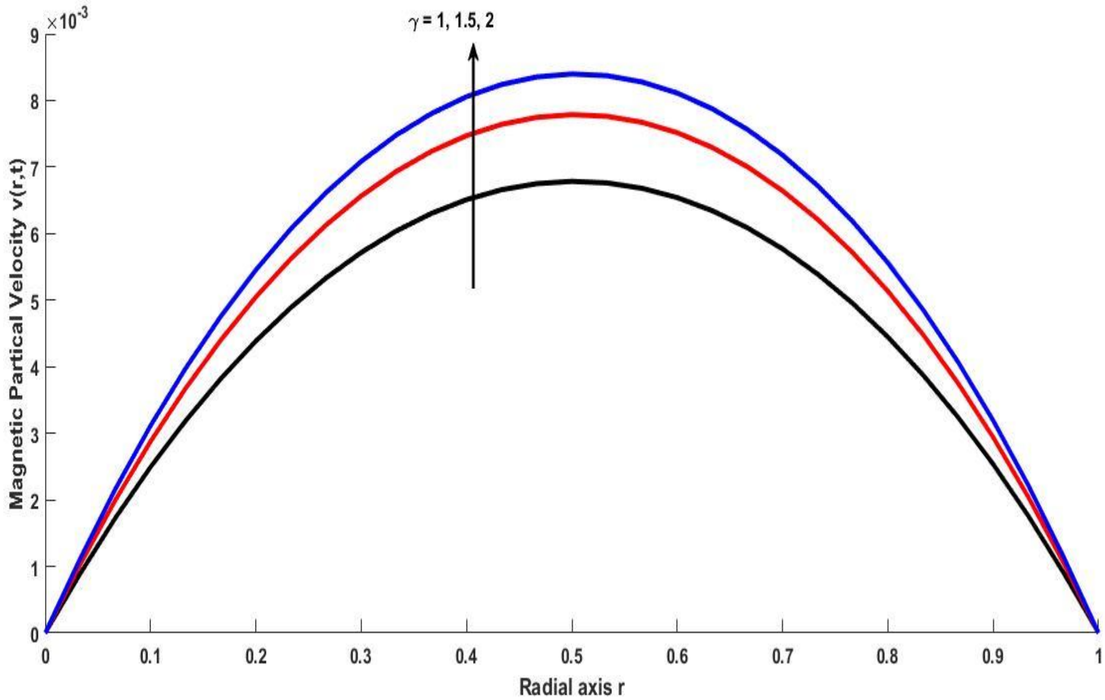

Fig. 5: γ on Magnetic Particle Velocity

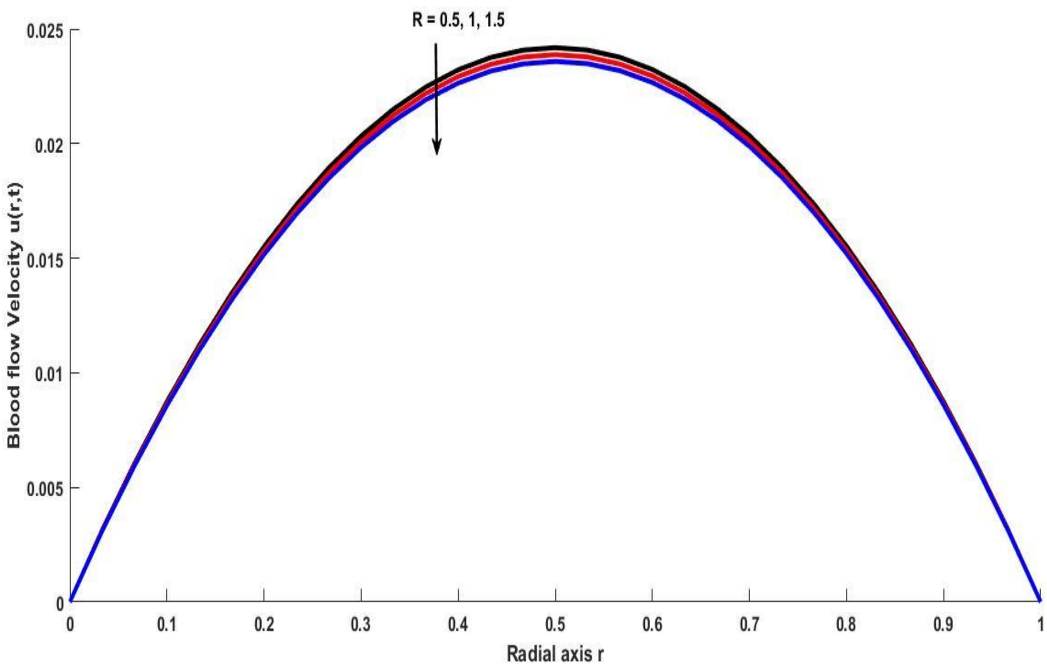

Fig. 6: R on Blood Velocity

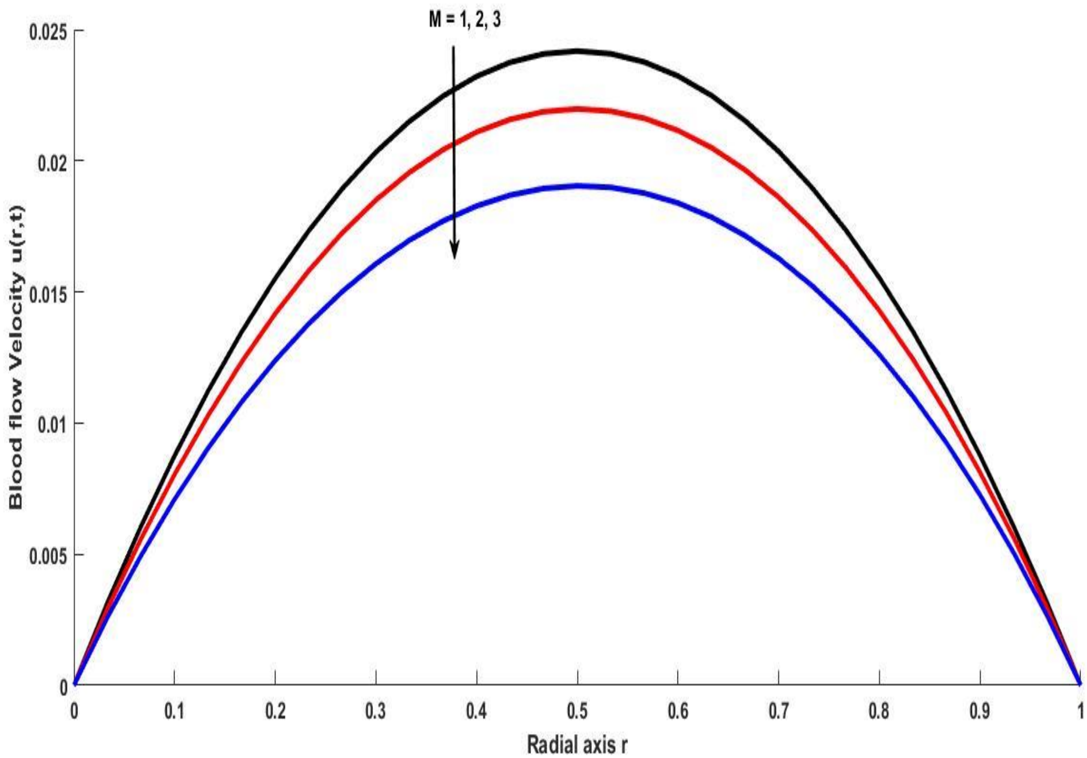

Fig. 7: M on Blood Velocity

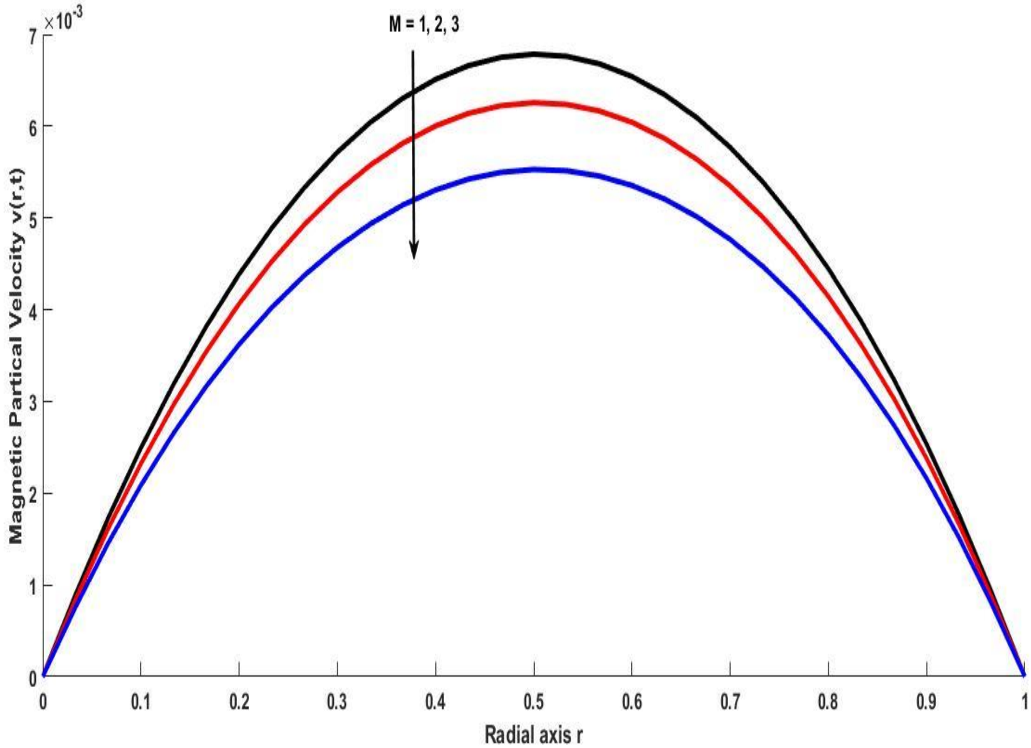

Fig. 8: M on Magnetic Particle Velocity.

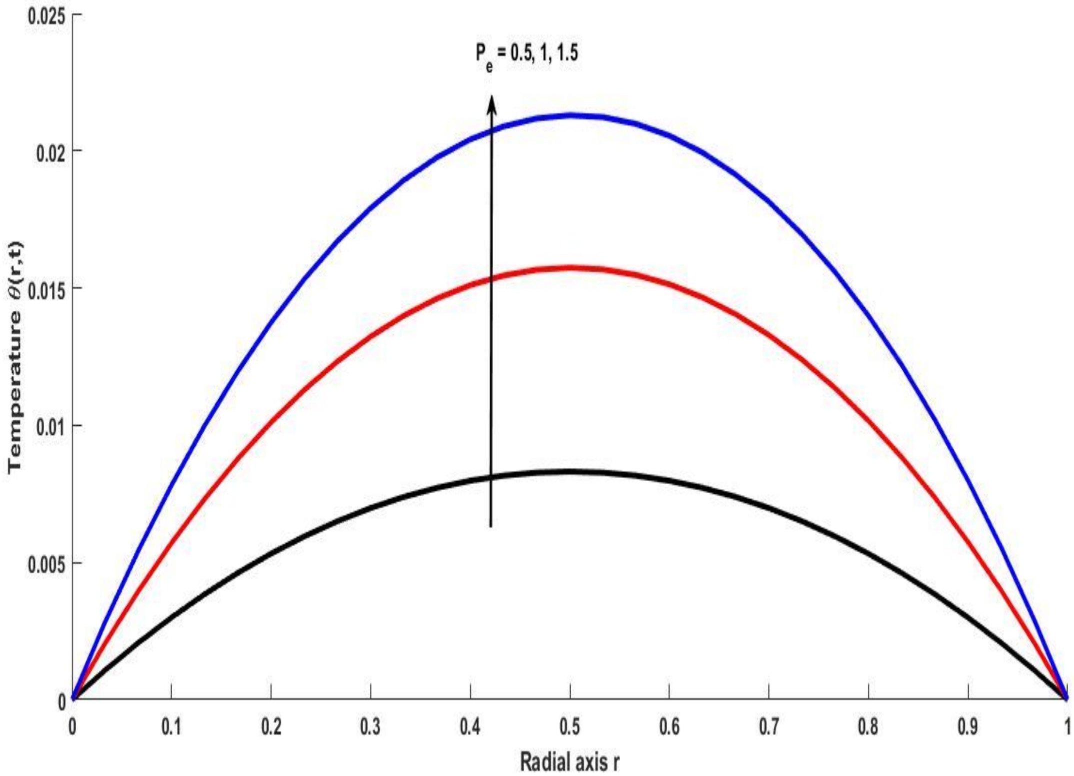

Fig. 9: P_e on Temperature.

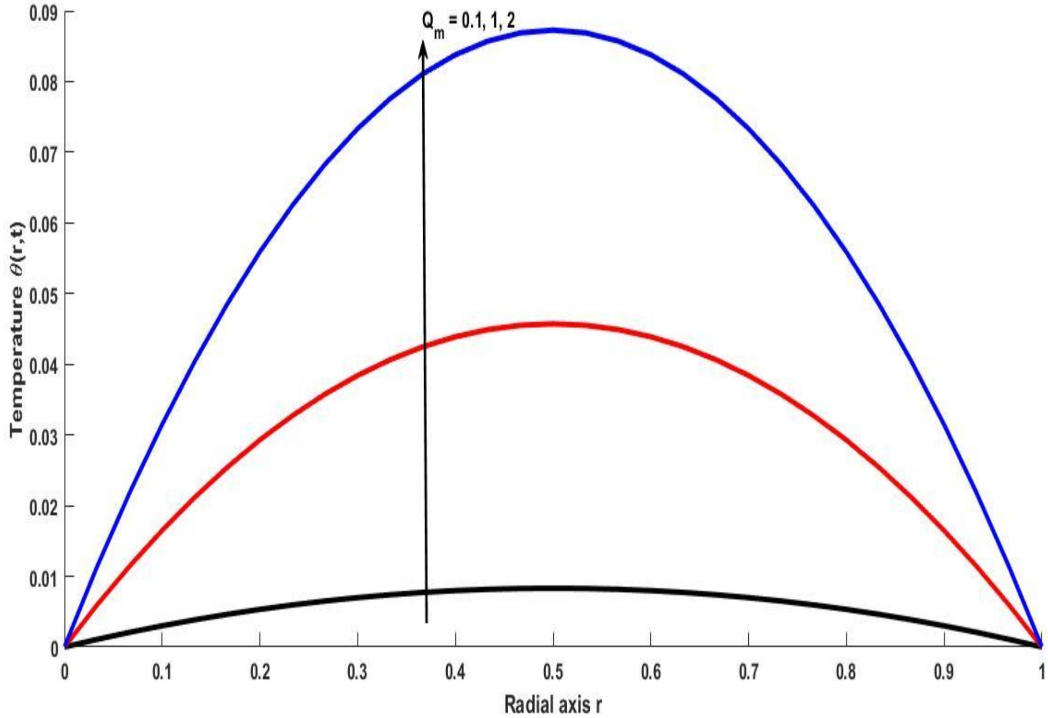

Fig. 10: Q_m on Temperature

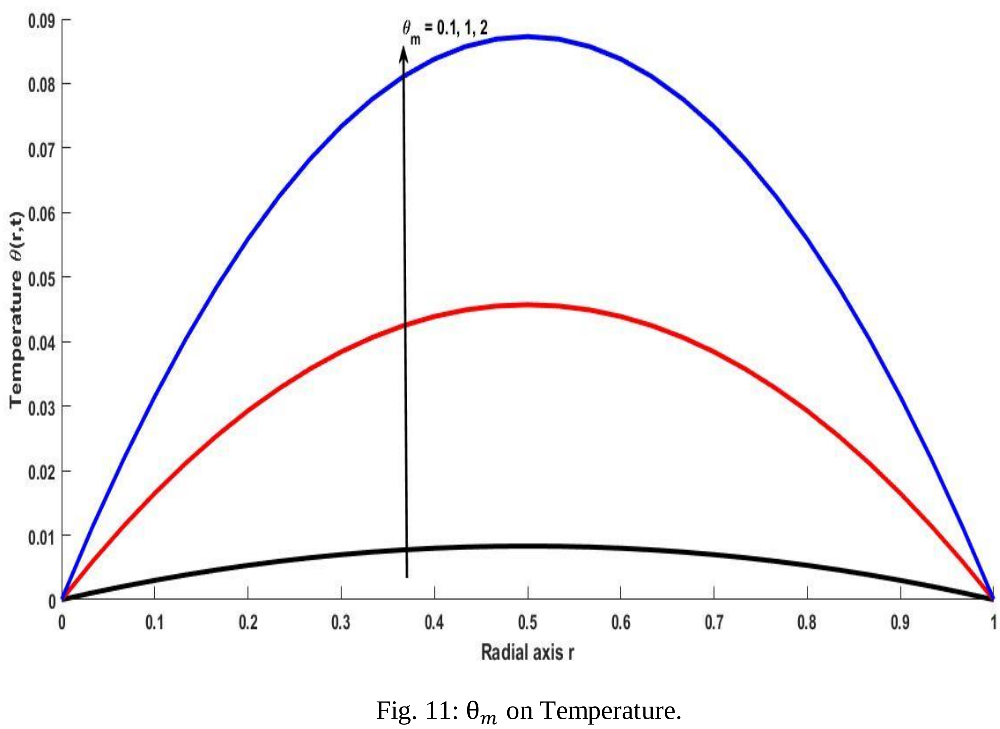

Fig. 11: θ_m on Temperature.

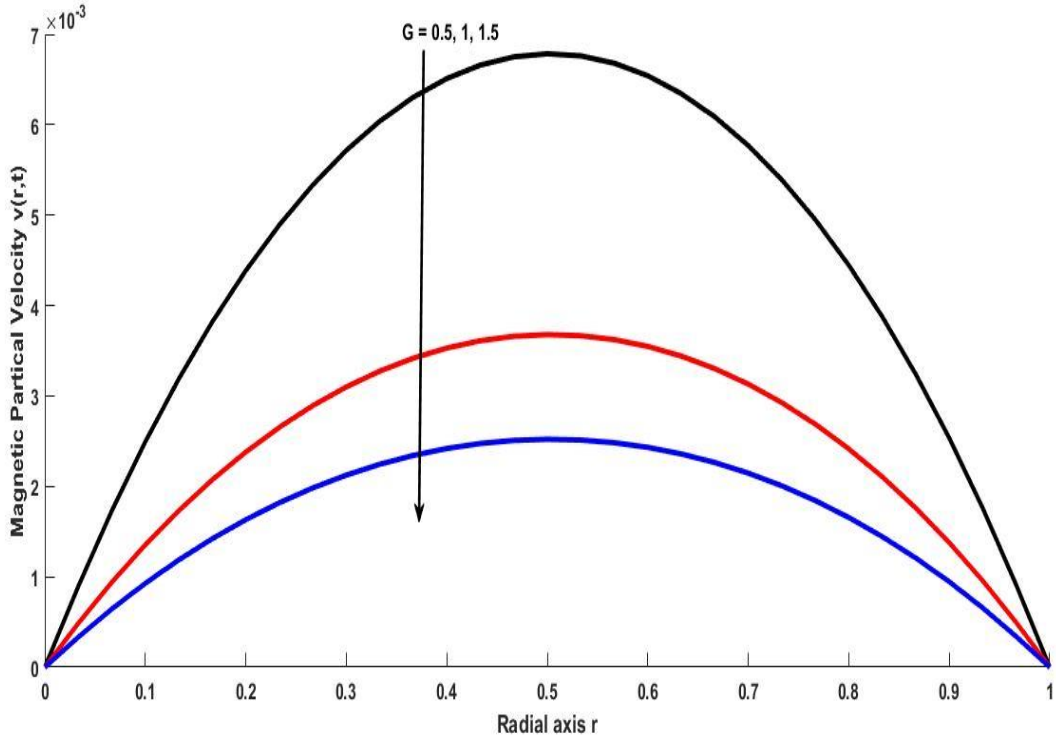

Fig. 12: G on Magnetic Particle Velocity.

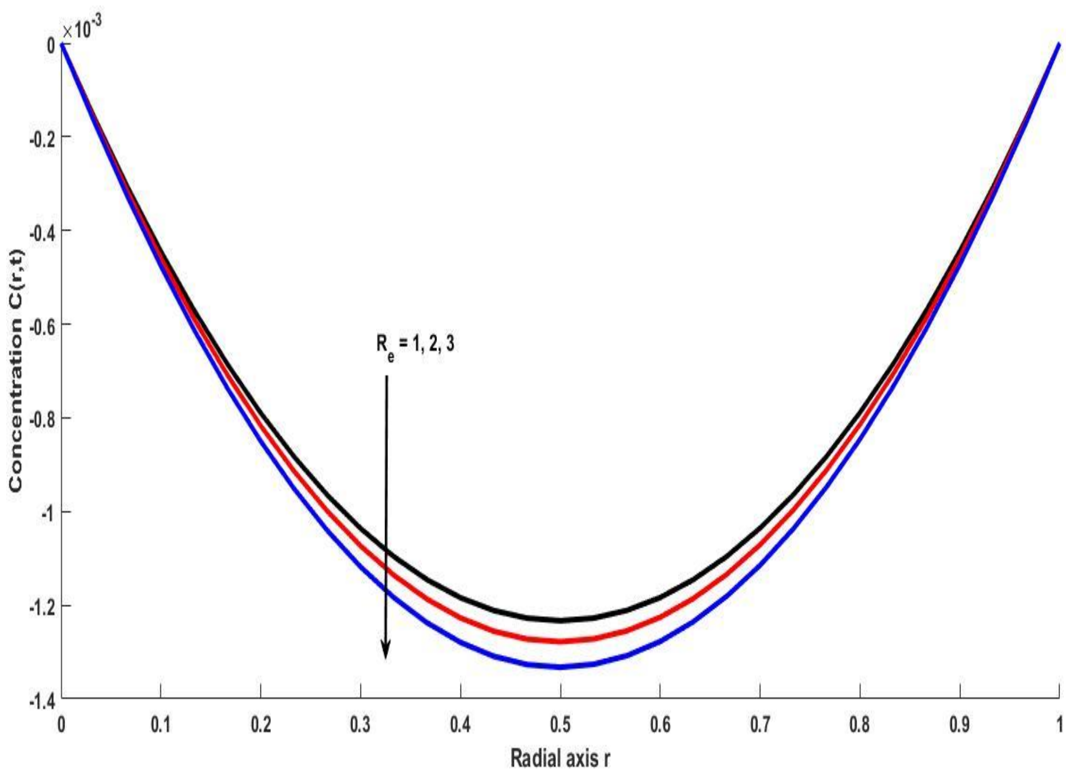

Fig. 13: R_e on Concentration

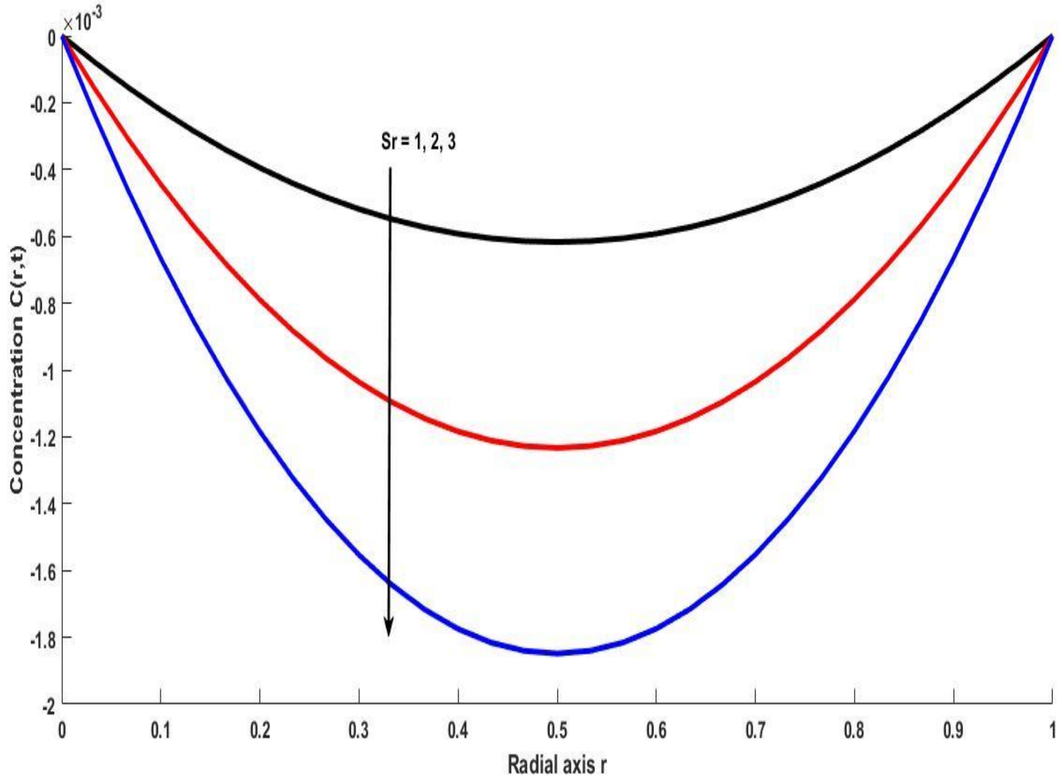

Fig. 14: Sr on Concentration

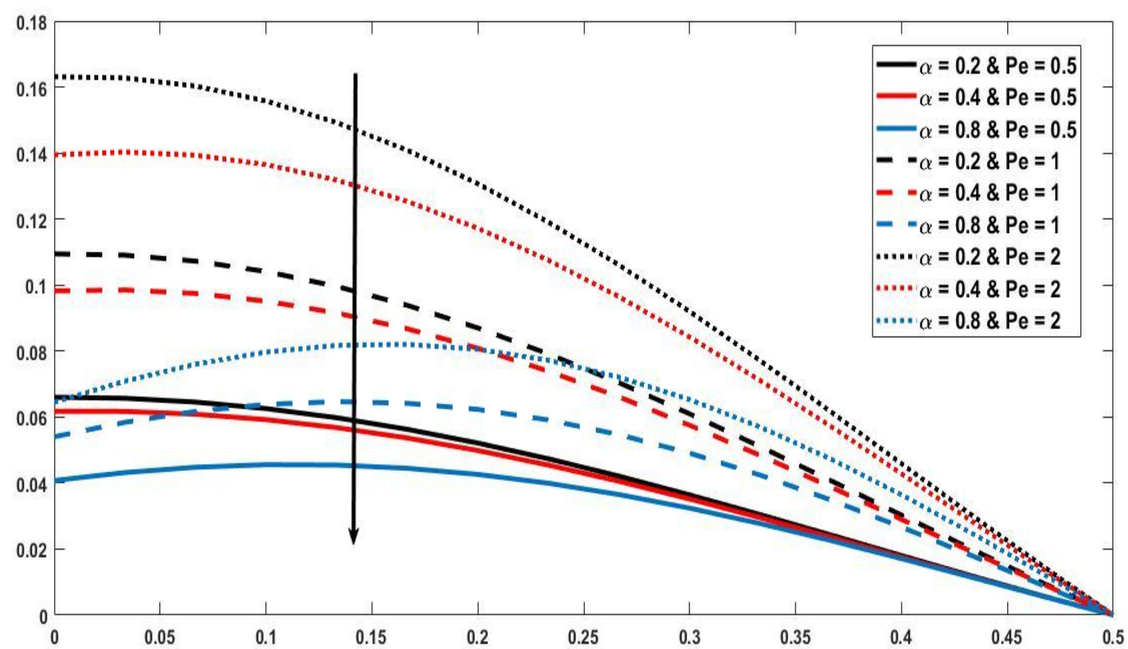

Fig. 15: α & P_e on Temperature

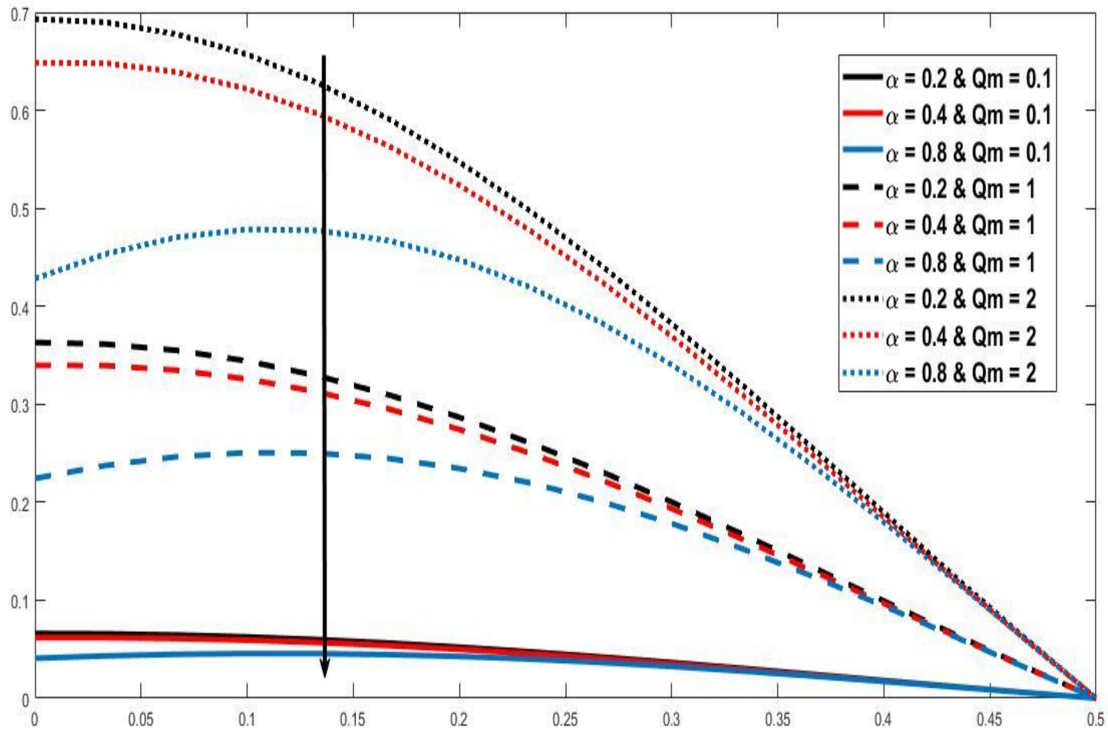

Fig. 16: α & Q_m on Temperature

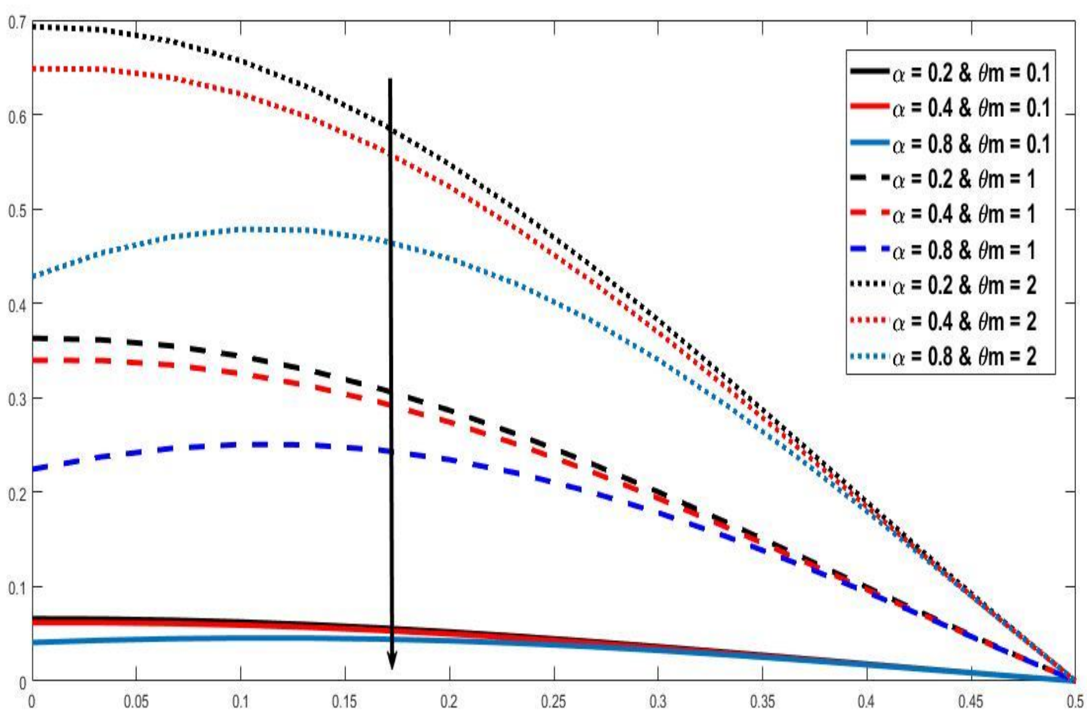

Fig. 17: α & θ_m on Temperature

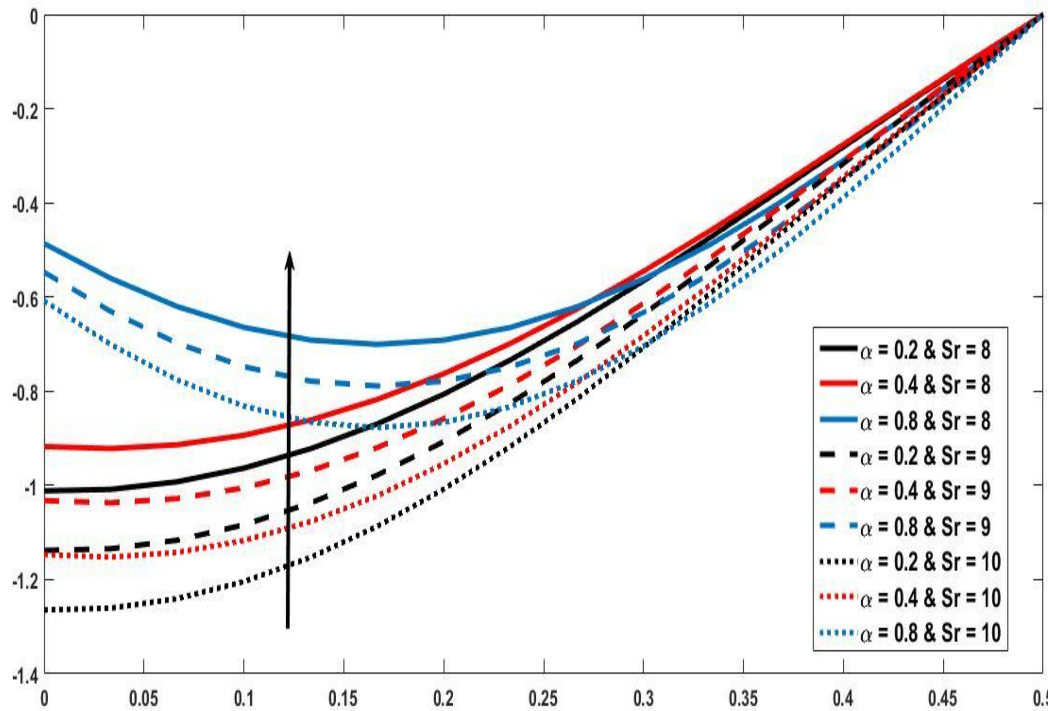

Fig. 18: α & Sr on Concentration

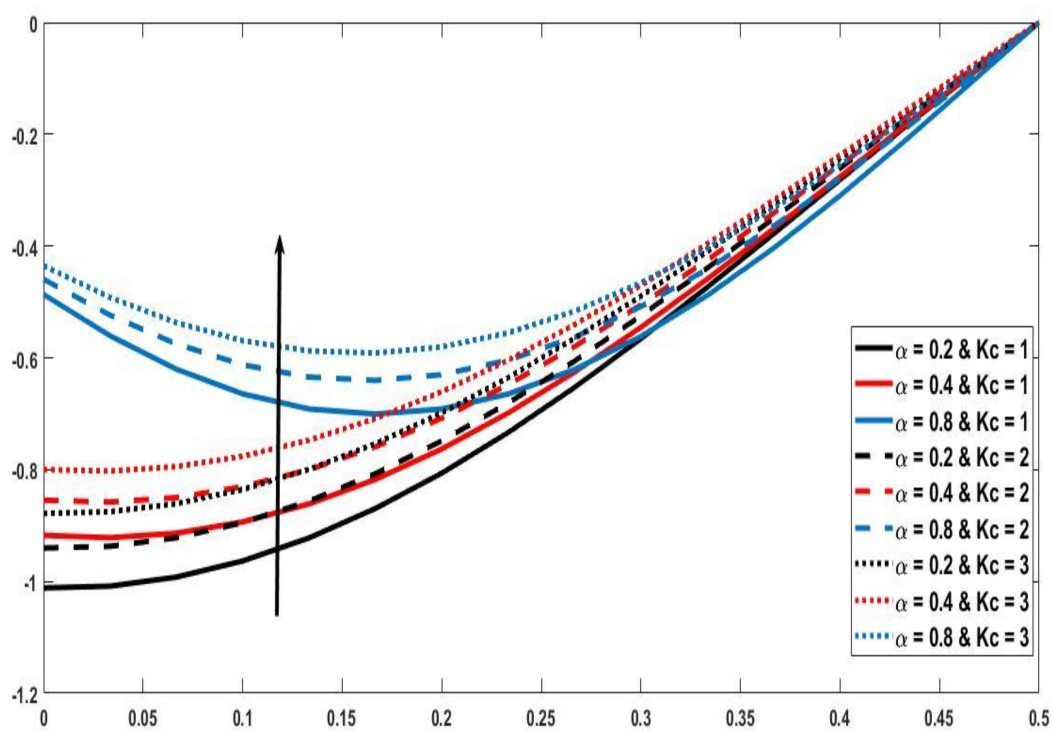

Fig. 19: α & K_c on Concentration.

Fig. 6 show the particle concentration R tends to reduce the motion of the flow. Physically, when we increase the value of R the thickness of the fluid is increase. The effects of external magnet on blood and magnetic particle velocity which is describe in Fig. 7 to 8. From the Figure and physical point of view, magnetic fields tend to reduce the motion of the blood flow. Figure 9 show the Prandtl number effects on temperature profiles. Physically, thermal diffusivity gives the measurement of how the temperature will be changed when it is cold or heated. Form the figures, it is concluded that the increases the thermal diffusivity, the heat transfer process is raised as well as motion of both flow is also improved. If thermal diffusivity is more, then heat diffusion is less. Fig. 10 to 11 show the effects of heat generation and absorption parameter on blood velocity, magnetic particle velocity and temperature profiles. Because of heat generation, heat transfer process is increase and motion of blood and magnetic particle become raised. These results agree with real situation because when we increase the value of heat generation, the fluid become thinner and so fluid is more accelerated. The size of the particles is what determines the value of the parameter for the particle mass known as G. According to Fig. 12, the magnetic particle velocity tends to decrease as the mass parameter is increased. As shown in Fig. 13, concentration profiles vary with the Reynolds number. The Reynolds number is inversely proportional to the fluid's concentration profiles. The fluid's velocity gradually increases as Reynold's number rises whereas, the concentration decreases. Physically, lower viscosity (increased velocity) will increase. Fig. 14 show the effects of thermos-diffusion on concentration profiles. It is seen that the mass transfer process delayed with both parameters. This result is strongly agreement with published works. Fig. 15 to 19 indicate the effects of fractional derivative parameter α on temperature and concentration parameter. From all figures, it is concluded that the heat transfer process delayed whereas, improve the mass transfer process with increasing the value of $\alpha = 0.2, \alpha = 0.4, and\ \alpha = 0.8$ It is indicated that the fractional derivative is important phenomena to understanding the nature of fractional derivative.

4. Conclusion

The following are the key findings of the current study.

- It is notable that the axial velocity of blood flow can be reduced by applying magnetic field of the correct strength. This method can be used to treat hypotension by bringing the patient's blood pressure up to a healthy level. Magnetic fields at different angles effectively reduce strokes, swellings, and pains. The effects of magnetic fields on blood flow which leads to change the viscosity, which is helpful for controlling the motion of fluid.
- The systolic pressure gradient and diastolic pressure gradient tends to improve the blood velocity. Due to these effects, the flow of blood may be in normal form in stenosis artery.
- Heat generation tends to improve the heat transfer process as well as blood flow.
- The concentration level of the fluid rises with the falls due to the thermos-diffusion. This result will be important to investigate during cancer hyperthermia treatment.
- Fractional order parameter α tends to delay the heat transfer process whereas, improve the mass transfer process.

Appendix:

$B_1 = R + Ha^2 + B_1 r_n{}^2$

$B_2 = 1 + G - \alpha - R - R\alpha^2 + 2R\alpha + B_1 + B_1\alpha^2 - 2\alpha B_1 + GB_1 - G\alpha B_1$

$B_3 = \alpha + 2R\alpha^2 - 2R\alpha - 2B_1\alpha^2 + 2\alpha B_1 + G\alpha B_1$

$B_4 = B_1\alpha^2 - R\alpha^2, B_5 = 1 + \alpha^2 - 2\alpha + G + G\alpha\ , B_6 = -2\alpha^2 + 2\alpha + G\alpha$

$B_7 = \frac{-B_3 \pm \sqrt{B_3{}^2 - 4B_2B_4}}{2B_2}, B_8 = \frac{-B_3 \pm \sqrt{B_3{}^2 - 4B_2B_4}}{2B_2}, B_9 = \frac{B_7{}^2B_5 + B_7B_6 + \alpha^2}{B_7 - B_8},$

$B_{10} = \frac{B_8{}^2B_5 + B_8B_6 + \alpha^2}{B_8 - B_7}, B_{11} = (r_n)(1 - \alpha) + P_e, B_{12} = (r_n).\alpha$

$$B_{13} = P_e \frac{(Q_m + \theta_m)(1-\alpha)}{B_{11}}, B_{14} = P_e \frac{(Q_m + \theta_m).\alpha}{B_{11}}, B_{15} = \frac{B_{12}}{B_{11}},$$

$$B_{16} = -S_r\, S_c\, r_n P_e\, (Q_m + \theta_m), B_{17} = r_n, B_{18} = r_n + S_c\, K_c\, R_e^2,$$

$$B_{19} = R_e S_c\,, B_{20} = B_{17} - B_{17}\alpha + P_e, B_{21} = B_{19} + B_{18} - B_{18}\alpha, B_{22} = B_{17}\alpha$$

$$B_{23} = B_{18}\alpha, B_{24} = \frac{B_{16}}{B_{20}.B_{21}}, B_{25} = 2\alpha(1-\alpha), B_{26} = (1-\alpha)^2, B_{27} = \frac{B_{22}}{B_{20}}$$

$$B_{28} = \frac{B_{23}}{B_{21}}, B_{29} = \frac{B_{24}(\alpha^2)}{B_{27}B_{28}}, B_{30} = \frac{B_{24}(\alpha^2 + B_{25}(-B_{27}) + B_{26}(B_{27})^2)}{(-B_{27})(B_{28} - B_{27})},$$

$$B_{31} = \frac{B_{24}(\alpha^2 + B_{25}(-B_{28}) + B_{26}(B_{28})^2)}{(-B_{28})(B_{27} - B_{28})}, B_{32} = \frac{1-\alpha}{G-\alpha+1}, \quad B_{33} = \frac{\alpha}{G-\alpha+1}$$

$$f * g - \text{convolution of } f \,\&\, g\,, f * g = \int_0^t f(z)g(t-z)dz$$

References:

[1] Kollin, A. "Electromagnetic flowmeter: Principle of method and its application to blood flow measurement." Proc. Soc. Exp. Biol. Med 35 (1936): 53.

[2] Korchevskii, E. M., and L. S. Marochnik. "Magnetohydrodynamic version of movement of blood." Biophysics 10, no. 2 (1965): 411-414.

[3] Vardanyan, V. A. "Effect of magnetic field on blood flow." Biofizika 18 (1973): 491-496.

[4] Abdullah, Ilyani, Norsarahaida Amin, and Tasawar Hayat. "Magnetohydrodynamic effects on blood flow through an irregular stenosis." International Journal for Numerical Methods in Fluids 67, no. 11 (2011): 1624-1636. **https://doi.org/10.1002/fld.2436**

[5] Bose, Sayan, and Moloy Banerjee. "Magnetic particle capture for biomagnetic fluid flow in stenosed aortic bifurcation considering particle–fluid coupling." Journal of Magnetism and Magnetic Materials 385 (2015): 32-46. https://doi.org/10.1016/j.jmmm.2015.02.060

[6] Ali, Farhad, Nadeem Ahmad Sheikh, Ilyas Khan, and Muhammad Saqib. "Magnetic field effect on blood flow of Casson fluid in axisymmetric cylindrical tube: A fractional model." Journal of Magnetism and Magnetic Materials 423 (2017): 327-336. https://doi.org/10.1016/j.jmmm.2016.09.125

[7] Pennes, Harry H. "Analysis of tissue and arterial blood temperatures in the resting human forearm." Journal of applied physiology 1, no. 2 (1948): 93-122.

[8] Barnothy, Madeleine F., and I. Sümegi. "Effects of the magnetic field on internal organs and the endocrine system of mice." In Biological effects of magnetic fields, pp. 103-126. Springer, Boston, MA, 1969. https://doi.org/10.1007/978-1-4684-8352-9_7

[9] El-Sayed, M. F., N. T. M. Eldabe, A. Y. Ghaly, and H. M. Sayed. "Effects of chemical reaction, heat, and mass transfer on non-Newtonian fluid flow through porous medium in a vertical peristaltic tube." Transport in porous media 89, no. 2 (2011): 185-212. https://doi.org/10.1007/s11242-011-9764-3

[10] Hayat, T., M. Ijaz Khan, M. Waqas, A. Alsaedi, and Muhammad Imran Khan. "Radiative flow of micropolar nanofluid accounting thermophoresis and Brownian moment." International Journal of Hydrogen Energy 42, no. 26 (2017): 16821-16833. https://doi.org/10.1016/j.ijhydene.2017.05.006

[11] Ganesan, P., and G. Palani. "Finite difference analysis of unsteady natural convection MHD flow past an inclined plate with variable surface heat and mass flux." International journal of heat and mass transfer 47, no. 19-20 (2004): 4449-4457. https://doi.org/10.1016/j.ijheatmasstransfer.2004.04.034

[12] Takhar, Harmindar S., Ali J. Chamkha, and Girishwar Nath. "Unsteady laminar MHD flow and heat transfer in the stagnation region of an impulsively spinning and translating sphere in the presence of buoyancy forces." Heat and Mass Transfer 37, no. 4 (2001): 397-402. https://doi.org/10.1007/s002310100227

[13] Abbas, Zaheer, Jafar Hasnain, and Muhammad Sajid. "MHD two-phase fluid flow and heat transfer with partial slip in an inclined channel." Thermal Science 20, no. 5 (2016): 1435-1446. https://doi.org/10.2298/TSCI130327049A

[14] Khaled, A-RA, and Kambiz Vafai. "The role of porous media in modeling flow and heat transfer in biological tissues." International Journal of Heat and Mass Transfer 46, no. 26 (2003): 4989-5003. https://doi.org/10.1016/S0017-9310(03)00301-6

[15] Shah, Nehad Ali, Dumitru Vieru, and Constantin Fetecau. "Effects of the fractional order and magnetic field on the blood flow in cylindrical domains." Journal of Magnetism and Magnetic Materials 409 (2016): 10-19. https://doi.org/10.1016/j.jmmm.2016.02.013

[16] Mondal, M., Biswas, R., Hasan, M., Kazi Shanchia, M., Ahmmed, S. F., International journal of heat and technology, 37 (1) (2019) 59-70. DOI: https://doi.org/10.18280/ijht.370107

[17] Biswas, R., Mondal, M., Hossain, S., Kazi Farhin Urmi, U. K. Suma, M. Katun, Advanced Science, Engineering and Medicine, 11 (2019) 687-696. https://doi.org/10.1063/1.5115852

[18] Kataria, H. R., Patel, H. R., Heat and mass transfer in MHD Casson fluid flow past over an oscillating vertical plate embedded in porous medium with ramped wall temperature, Propulsion and Power Research, 7 (3) (2018) 257-267. https://doi.org/10.1016/j.jppr.2018.07.003

[19] Maiti, S., S. Shaw, and G. C. Shit. "Caputo–Fabrizio fractional order model on MHD blood flow with heat and mass transfer through a porous vessel in the presence of thermal radiation." Physica A: Statistical Mechanics and its Applications 540 (2020): 123149. https://doi.org/10.1016/j.physa.2019.123149